Journal of Bioscience and Bioengineering
VOL. 114 No. 1, 113–120, 2012

www.elsevier.com/locate/jbiosc

Regulated patterns of bacterial movements based on their secreted cellulose nanofibers interacting interfacially with ordered chitin templates

Tetsuo Kondo,[1,*] Wakako Kasai,[1] Masanobu Nojiri,[2] Yukako Hishikawa,[2] Eiji Togawa,[2] Dwight Romanovicz,[3] and R. Malcolm Brown Jr.[3]

Graduate School of Bioresource and Bioenvironmental Sciences, Kyushu University, 6-10-1 Hakozaki, Higashi-ku, Fukuoka 812-8581, Japan,[1] Forestry and Forest Products Research Institute (FFPRI), 1 Matsunosato, Tsukuba, Ibaraki 305-8687, Japan,[2] and School of Biological Sciences, Section of Molecular Genetics and Microbiology, The University of Texas at Austin, Austin, Texas 78712, USA[3]

Received 26 October 2011; accepted 21 February 2012
Available online 9 May 2012

***Gluconacetobacter xylinus*, a gram-negative bacterium that synthesizes and extrudes a cellulose nanofiber in SH media moves in random manners, resulting in 3D-network structure of the secreted nanofibers termed a pellicle. In this study, the bacterial movement was successfully regulated to be in a waving manner when cultured on ordered templates made of chitin. Interestingly, by addition of more cellulose into the chitin ordered templates, the waving pattern was getting close to a linear or straight manner. Real time video analysis and other visualization techniques clarified that the regulation of the moving manners was due to the interfacial interaction between the secreted nanofibers and the template surfaces. Furthermore, the changing of the pattern due to the cellulose content in the ordered templates appeared to depend on the magnitude of the interaction between the template and nanofibers. This regulated autonomous deposition of the fibers will build patterned 3D-structure with unique properties on the surface of the templates, leading to a novel type of nanotechnology using biological systems with biomolecular nano-templates to design 3D-structures.**

[**Key words:** *Gluconacetobacter xylinus*; Directed nano-patterning; Chitin; Cellulose; Nematic ordered cellulose; Nano-engine; Autonomous fabrication; Ordered template]

Attempts to understand interfacial surface structures and the interaction of materials at the nanoscale have brought us into the field of nanotechnology (1). Microbiological systems combined with nanotechnology have become bio-nanotechnology (2). Recent studies showing the unique interaction of biological systems with entirely synthetic molecular assemblies have prompted consideration of a new generation of approaches for controlled nano-assembly. More recently, we found a unique phenomenon that the molecular tracks of nematic ordered cellulose (NOC) (3) substrate regulated the direction of fiber secretion of *Gluconacetobacter xylinus*, a gram-negative bacterium that synthesizes and extrudes a cellulose nanofiber, resulting also in regulating the direction of the bacterial movement caused by the inverse force of the secretion. An epitaxial deposition of the nanofibers was induced due to the strong interaction between the nascent nanofibrils and influenced the order of molecules of the template (4). This indicated that the conjunction of directed biosynthesis and the ordered fabrication from the nano to the micro scales could lead to new methodologies for design of functional materials with desired nanostructures.

In the unique phenomenon, the most influential factor for the regulated bacterial movement was the surface of the nano/micro structure of the template. The NOC substrate where cellulose molecules are highly ordered, but not assembled to form the crystalline state, was prepared by uniaxial stretching of water-swollen cellulose gel from the dimethyl acetamide/LiCl solution. Under these conditions, the cellulose molecular chains tend to be oriented toward the stretching axis. Simultaneously, the hydroxyl groups at the C-6 position that are equatorial-bonded to the anhydroglucose unit in the cellulose molecules are automatically oriented at a certain angle against the surface and also aligned along the same axis as the tracks (5). On the contrary, the lateral order of the OH groups is not well coordinated because of the molecular chain movements with each other in the NOC that was caused by the uniaxial stretching. Therefore, the OH groups tend to be oriented as molecular tracks only in one direction across the entire NOC surface (3,5). These ordering tracks of the OH groups on the NOC surface appear to induce epitaxial deposition of the biosynthesized cellulose nanofibers as they are secreted from *G. xylinus* along the same axis of the tracks in NOC. In addition, the regulated movement of the bacterium was not observed in the synthetic polymers having OH groups such as poly (vinyl alcohol) (4). Therefore, when the nematic ordered state is prepared using other natural polymers, it is of interest and importance to know whether the similar regulated bacterial movement may occur in order to extend this phenomenon into

* Corresponding author. Tel./fax: +81 92 642 2997.
E-mail address: tekondo@agr.kyushu-u.ac.jp (T. Kondo).

1389-1723/$ – see front matter
doi:10.1016/j.jbiosc.2012.02.020

a methodology for fabrication of new types of functional bio-based materials.

In the present work, we employed chitin and cellulose/chitin blends as the components for the above templates instead of NOC. Chitin is a repeating carbohydrate polymer of (1,4) linked 2-deoxy-2-acetamide-β-D-glucose. Namely, as the primary structure, chitin has only a replacement of hydroxyl groups into acetamide groups at the C-2 position of anhydroglucose unit when compared with cellulose molecule. However, when treated in the same manner as with NOC, the chitin exhibited a variety of different micro/nano hierarchical nematic ordered states from those reported in our previous paper (6). Therefore, when each nematic ordered chitin and chitin/cellulose template is used as a template for the regulation of the bacterial movement and nanofiber deposition, it has been found to provide a unique patterning of the bacterial movement and deposition of their secreted cellulose nanofibers. This phenomenon allows development of new patterns of ordered sheet structures. Furthermore, this unique relationship between directed biosynthesis and the regulated fabrication could lead to the design of 3-D architecture from the nano to the micro scales of functional bio-based materials with desired patterned nanostructures.

MATERIALS AND METHODS

Materials α-Chitin samples were provided by Katakura Chikkarin Co. Ltd., and purified according to a previous paper (7). The cellulose and α-chitin were first dried under vacuum at 40°C. *N,N*-Dimethylacetamide (DMAc) purchased from Katayama Chemicals Co. Ltd. (99+%) was dehydrated with molecular sieve 3A and used without further purification. Lithium chloride (LiCl) powder (Katayama Chemicals Co. Ltd.) was oven-dried at least for 3 days at 105°C.

Preparation of nematic ordered chitin templates in Schramm–Hestrin (SH) medium Dissolution of cellulose and α-chitin and the subsequent preparation of water-swollen gel films were basically followed by a previous swelling procedure using a solvent exchange technique (6,8).

Nematic ordered chitin templates were prepared according to the previous methods (3,6). Basically nematic ordered films were prepared by stretching water-swollen gel-like films above prepared. The films were cut into strips approximately 30 mm long and 5 mm wide. The water-swollen strips were then clamped in a manual stretching device and elongated uniaxially to a draw ratio of 2.0–2.3 (minimum-required over 2.0) at room temperature. The entire drawing process was completed while the specimen was still in a wet state. Following air-drying, the drawn specimen in the stretching device was vacuum-dried at 40–50°C for more than 24 h. The thickness of the dried films for X-ray measurements was about 80 μm.

Nematic ordered blend films of α-chitin and cellulose were prepared as follows (6): DMAc/LiCl was used as the common solvent for all samples to be mixed. Concentrations of the solution were 1 wt% for both cellulose and chitin. All solutions were filtered and stored in a closed container. Separately prepared solutions of the chitin and cellulose were mixed at room temperature in the desired proportions. The relative composition of the two polymers in the mixed solutions was 100/0, 75/25, 50/50, 25/75 and 0/100 by weight (chitin/cellulose), respectively. After stirring for more than 3 days, the mixed solutions were used to prepare nematic ordered blend films by coagulation. The slow coagulation to prepare the gel-like film from a DMAc/LiCl solution was carried out according to the previous technique (3–6,8). The solution was poured into a surface-cleaned glass Petri dish with a flat bottom and placed in a closed box containing saturated water vapor at room temperature. In the blend solution, saturated water vapor slowly diffusing into the solution was employed to precipitate the chitin/cellulose blend gel. It was allowed to stand at room temperature for a few days until precipitation under a saturated water vapor atmosphere was complete to obtain the gel-like film. The precipitated gel-like film (at this stage fixation of the film appeared to be completed) was washed thoroughly with water to remove the solvent, and then the film was put in water to exchange the solvent in order to obtain a water-swollen transparent gel-like film. This water-swollen chitin/cellulose blended film was stretched in the same manner for NOC to be formed into nematic ordered blended films.

Then the above-prepared never-dried chitin and the blend with cellulose templates were put into Schramm–Hestrin (SH) medium (9) at pH 6.0, and the solvent was exchanged and finally maintained in a Petri dish until used for the study.

Bacterial cultures *G. xylinus* (=*Acetobacter xylinum*) (NQ-5: ATCC53582) was cultured in Schramm–Hestrin (SH) medium at pH 6.0 under 30°C atmosphere (9). After 3 days' cultivation, the synthesized pellicle was removed, and the remaining medium solution was stirred using a mixing instrument (Vortex) to obtain the active bacteria.

Measurements and analyses X-ray diffraction measurements were basically performed according to our previous reports (3,8). Wide angle X-ray diffraction (WAXD) patterns were taken by a transmission method using Ni filtered CuKα radiation produced by a Rigaku RINT-2500HF X-ray generator. WAXD patterns were measured at 40 kV and 200 mA with scanning speed of 0.5°/min and scan step of 0.02°, and recorded on a imaging plate (Fuji Film BAS-SR, 127 mm × 127 mm) at 40 kV and 60 mA for 10 min with a camera length of 60 mm, then analyzed with a Rigaku R-AXIS-DS3 system.

The WAXD intensity curves with a scanning speed of 0.5°/min were measured by a transmission method using a scintillation counter at 40 kV and 200 mA through the angular range 2θ for the equatorial and the meridional scans to the drawing direction; 2θ = 5–35° and 10–40°, respectively. Instrumental broadening was corrected using Si powder as a standard. The crystallinity from the WAXD intensity curve was calculated assuming that the area ratio was given by the crystalline region area divided by the total areas. To avoid complications due to contributions from the sample orientation in this measurement, the sample was cut into small pieces (a coarse powder) that were placed in a 1 mm glass capillary tube. The crystallite orientation parameter π, for drawn films was estimated followed by the previous method using Eq. 1 (3,8):

$$\pi = (180 - H^{\circ})/180 \quad (1)$$

where H° is the half-width of the azimuthal intensity distribution for the meridional reflection at 35°.

For sample specimens examined by high-resolution transmission electron microscopy, the cellulose solutions were also prepared in the same way as described above and diluted 100 times with water-free DMAc (1.0×10^{-2} wt%). After the solution covered a 3.0 mm TEM grid without coating, the grid was left for more than 3 days at room temperature under a saturated water vapor. During this period, a cellulose or chitin gel-like film was precipitated and at the same time was naturally stretched across the 3.0 mm diameter of the TEM grid. It was then washed thoroughly with distilled water to exchange the solvent prior to the addition of the negative staining agent (aqueous 2% uranyl acetate) and finally air-dried. Interaction with uranyl acetate appears to protect samples from electron beam damage (3). Specimens were observed with a Philips EM 420 transmission electron microscope operated at 100 kV with a beam current less than 5 μA. TEM images were acquired at magnifications of 210 K and 450 K using a GATAN Model 622 camera. The magnification factor for conversion to the digital image was 23×. The images were digitized, saved, and processed by Image Pro Plus software v.4.1 (Media Cybernetics).

AFM images of the cellulose film specimens were acquired on a Nanoscope IIIa (Digital Instruments) microscope. AFM was performed at room temperature, being controlled in contact (DC) mode with a scan rate from 1 to 3 Hz to observe $1 \times 1\ \mu m^2$ areas. The AFM tip employed was an etched-silicon AFM tip with a nominal radius from 5 to 15 nm, a cone angle of 35° and a height of about 15 μm which was mounted on a rectangular type cantilever with a spring constant of 0.13 Nm^{-1}. The scanning was carried out in both directions of the stretching axis of the film and perpendicular to the axis. The width and height of the aggregates was measured using a cross-sectional line profile analysis. Since the width data included geometrical enhancement due to the tip radius, they can be corrected using an equation introduced previously (3–5). In our case, as the height of the aggregates was smaller than radius of the tip, the following correction equation was employed:

$$E = 2 \times \left(RH - H^2\right)^{1/2}, w = W - E \quad (2)$$

where E is geometrical enhancement on the real width value (w), W is apparent width observed in AFM, H is height of the object observed in AFM, and R is the AFM tip radius. In this study we employed the R value as 10 nm in radius.

For real time video analyses, light microscopy images were acquired with 20× or 40× objective lenses, coupled with a 1.6× optivar lens using a Zeiss light microscope with an Optronix cooled CCD camera, attached with a 0.55× camera lens (HR 055-CMT) from Diagnostic, Instruments, Inc. Frames were captured, digitized, saved, and processed using Image Pro Plus software v.4.1 (Media Cybernetics) at a rate which resulted in the acquisition of 1 frame/20 s (3 frames per minute). Samples observed were specimens of the bacteria on substrates, covered with SH medium kept just above the surface at 24°C. The focus of the camera was set between the bacteria and the surface of the substrates, so that both the bacteria and the synthesized cellulose nanofibers could be observed. Incident light in the system was minimized to prevent drying of the surface by the heat produced. Using Adobe Premier v5.1, each captured frame was sequenced to produce a movie at the rate of 30 fps.

The sample specimens for FE-SEM were prepared according to the following: (i) the sample was rapidly frozen at a desired stage with liquid nitrogen and then transferred to glutaraldehyde/acetone (2% w/v) at −80°C. After 3 days at −80°C and a slow warming to room temperature, the specimen was exchanged to ethanol then dried using a critical point drying device, mounted on a stab and coated with Au for FE-SEM observation; or, (ii) the sample at a desired stage was placed into a container with several drops of a 4% OsO_4/H_2O solution, so that osmium vapor could fix the sample. The specimen was dehydrated with an ethanol series (30%, 50%, 70%, 90%, 100%), then dried and coated as described above.

The samples prepared as described above were observed with a Hitachi S-4500 FE-SEM at 5 or 8 KV. The SEM images were acquired as digitalized *.tif files at 8 bit radiometric resolution. The images were processed (contrast enhancement,

calibration of the scale, statistical size data collection and cross-section along the desired line) by Image Pro Plus software v.4.1 (Media Cybernetics).

RESULTS AND DISCUSSION

Molecular ordering templates from α-chitin and chitin/cellulose blends to regulate bacterial movements During cellulose biosynthesis, *G. xylinus* was found to move at a rate of 2.0 μm per min at 25°C, due to an inverse force derived from the secretion of crystalline cellulose microfibrils by the bacterium (10). It is noted that when it is transferred on a nematic ordered cellulose (NOC) template, it moved faster by 4.5 μm per min at 25°C in contact with the template (4,5,11). Moreover, the growth of the microfibrils is directed along a certain orientation by contact with the template, as reported previously (4). We have recently found that such a growth induces the increase in height of the produced three-dimensional oriented cellulose structure as distant as 300 nm from the surface of that template (data not shown). In any case, the strong interaction between the NOC template with a uniaxial orientation and the secreted 3–4 nm nanofibrils allowed the bacterium to move and deposit the fibers following the direction of the molecular track (4). In these experiments, we explored altering the pattern of this simultaneous system using a chitin nematic ordered template instead of NOC.

Fig. 1 shows an image of the chitin template prepared in the same manner as the NOC template and observed with high-resolution electron microscopy (TEM) as well as atomic force microscopy (AFM). The two images exhibited apparently the orientation of molecular chains, but they were not clear enough to be estimated. To obtain the distance between individual molecular chains, selected oriented areas (shown in the rectangles of Fig. 1) of both high-resolution images were at first Fourier transformed to obtain the diffraction images. Then the manipulated diffraction images as seen in inserted images of Fig. 1 were inversely Fourier transformed back to the noise-canceled images shown in both bottom images of Fig. 1. In this way, the average distance between two parallel patterns in each image were provided for interpretation. As described previously, the chitin template thus prepared exhibited a variety of different micro/nano hierarchical nematic ordered states (6). Both observations indicate that the distance between individual lines (1.6 nm for TEM, 0.54 nm for AFM) is larger than the crystalline lattice constant of the *a* axis of α-chitin (a: 0.474 nm, b: 1.886 nm, c: 1.032 nm, $\alpha = \beta = \gamma = 90^\circ$) (12). Similarly to NOC, in which the glucan chain dimensions are 0.4–0.5 nm viewed from its narrow axis, AFM images with the chain width of 0.45 nm (see Fig. 1 right) clearly exhibit single molecular chains in the narrow axis on the surface of the chitin template. On the contrary, the TEM image may indicate a parallel alignment at a higher level of molecular assembly states, say microfibrils, described later. In any case, nematic ordered chitin was achieved, similar to our previous work with cellulose (3).

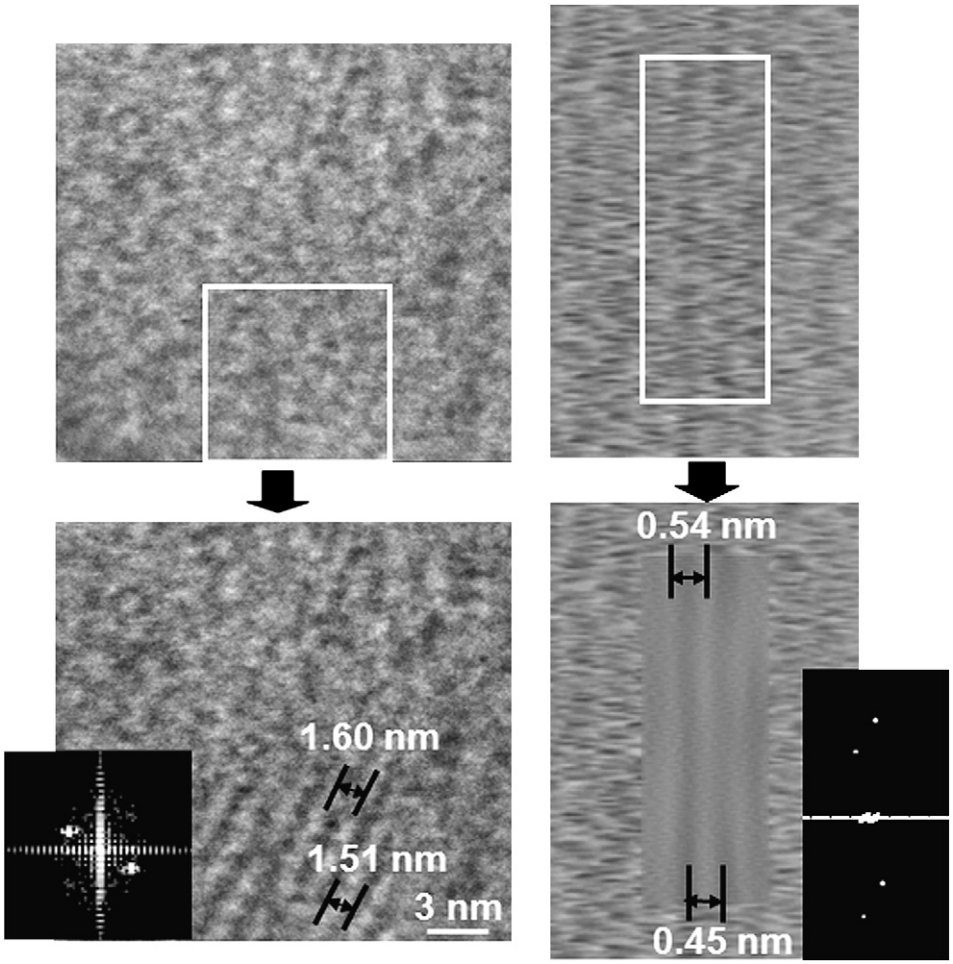

FIG. 1. An image of the chitin template prepared in the same manner as the NOC template; The left up was observed with high-resolution electron microscopy (TEM), the left bottom is an image manipulated by inverse Fourier transformation, the right up was observed with as atomic force microscopy (AFM), and the right bottom is an image manipulated by inverse Fourier transformation. The inserted images (both the left and right) are the manipulated diffraction images prior to inverse Fourier transformation.

Rates of bacterial movements on nematic ordered chitin templates When active *G. xylinus* cells were transferred to the nematic ordered chitin surface, they synthesized cellulose nanofibers (=cellulose ribbons) that are not parallel to the molecular orientation of the substrate, unlike the secreted fibers deposited on nematic ordered cellulose (NOC) templates. Instead, the bacteria begin to follow the molecular tracks, but soon they jump off the track, are detoured and then synthesize their cellulose parallel to neighboring tracks, once again soon jumping off. This waving pattern was repeated across the template, as evidenced by direct video imaging of the motion of the bacteria as they secrete the cellulose nanofiber, as shown in Fig. 2. This figure shows the time course (120 s between each frame) of the waving pattern of movement for a *G. xylinus* cell having 1 μm in width and 10 μm in length, respectively, together with the deposited fiber in the same waving pattern. The time lapse observation also provided that the cell movement was at a constant rate of 2.05 μm (standard deviation (SD) = ±0.14 μm)/min at 24°C as listed in Table 1, which is considered as the result of an inverse force imposed by the directed polymerization and crystallization of the cellulose in the bacterium. The amplitude and periodicity of the waving as indicated in Fig. 2 was 6.11 ± 0.53 μm and 17.85 ± 0.04 μm, respectively. As seen in the minimum standard deviation in the periodicity of the waving pattern, the movement of the bacterium was fairly periodical and regularized. However, the rate of motion on the nematic ordered chitin template was the same as that for cell movements without templates. Furthermore, there was no difference in the rate between movement on the track and off the track, indicating that the interaction of the nascent cellulose with the nematic ordered chitin template was not as strong as that with the NOC template. In nematic ordered chitin templates, hydrophilic hydroxyl groups at the C-6 position of glucopyranose ring and relatively hydrophobic acetamide groups at the C-2 position appeared alternately on the surface because of the 2_1 screw axis of the molecular chain, whereas the nematic ordered cellulose template provides only hydroxyl groups at the C-6 position on the surface. The balance of presence of the two substituents strongly affects the strength of the interaction between the surface and secreted cellulose microfibrils. When the contact with the chitin template is not as strong as that for nematic ordered cellulose, the biosynthesized individual sub-elementary fibrils (of a few nm in width) usually tend to be self-assembled to form a ribbon-type nanofiber with 40–60 nm in width. The situation when the bacteria secrete cellulose nanofibers cannot be changed without such a strong interaction between the interfaces. Accordingly, the rate of the deposition of the fibrils on the nematic ordered chitin template that corresponds to the rate of the bacterial movement did not change from the initial rate without the template (both the moving rates were 2.05 μm ± 5% at 24°C). On the contrary, when the interaction was strong enough like the case for the nematic ordered cellulose (NOC), the rate of movement on NOC was much higher when compared with movements on the templates composed of 100/0 (pure chitin) and 0/100 (pure cellulose) in Table 1. One explanation for this phenomenon is to determine the rate-determining step for both production of fibers and the bacterial movements. In our previous paper (11), it was assumed to be the self-assembly process of biosynthesized sub-elementary fibrils for forming a cellulose nanofiber. Namely in this case, the strong interfacial contact with the template prevented the assembly of the individual sub-elementary fibrils soon after the biosynthesis, resulting in inducing an increase in the rate, and also

TABLE 1. Statistic data for rates and patterns in the bacterial movements depending on composition of the nematic ordered chitin/cellulose blended templates.

	Composition of chitin/cellulose blends				
	100/0	75/25	50/50	25/75	0/100
Moving rate (μm/min at 24°C)	2.05 ± 0.14	2.93 ± 0.24	2.81 ± 0.63	2.12 ± 0.20	4.5[a]
Amplitude (μm)	6.11 ± 0.53	5.44 ± 0.97	3.92 ± 0.67	3.34 ± 0.51	0

[a] From Ref. 4.

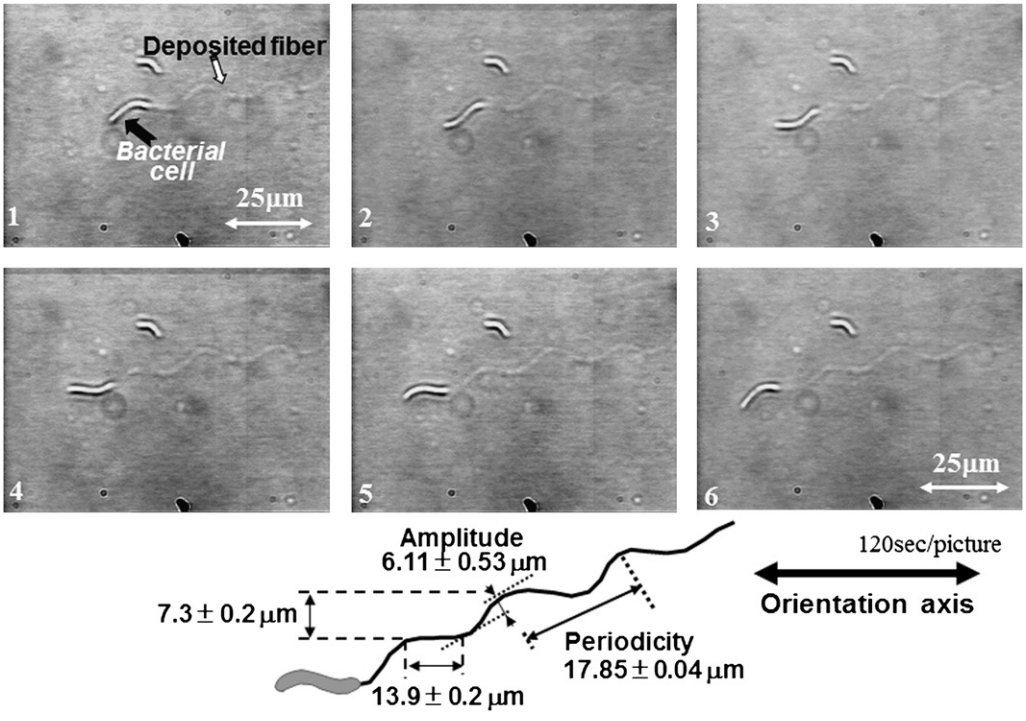

FIG. 2. Successive images showing the motion using real time video analysis of a bacterium as it secretes a cellulose nanofiber on the nematic ordered chitin template. The bacterium is attached, and thereafter synthesizing the fiber on the molecular tracks in the template to show a waving moving pattern. In this observation, the differential interference contrast microscopic mode was employed to clearly be seen for the secreted fibers as well as the bacterium.

could cause the release of stress for the enzymatic synthesis of cellulose. As the result, the production of fibers on the NOC template increases so as for the rate of bacterial movement as listed in Table 1 (see the value at 0/100). In fact, we previously found by FE-SEM observations that the bacterial sub-elementary fibrils extruded by the synthesizing enzymes could not self-assemble any more on the NOC template to form cellulose nanofibers, later becoming flattened by strongly attaching to the molecular tracks of OH groups on the template surface. This may have caused the prevention of self-assembly of the sub-elementary fibrils, and simultaneously an epitaxial nanodeposition along the molecular track direction on the surface of the template. It is also noted that the moving rate increased with increment of cellulose ratio and then decreased. This behavior may be due to a variety of different micro/nano hierarchical nematic ordered states depending on the cellulose content in the composited templates, as described later.

Patterning of fiber deposition on nematic ordered chitin templates revealed by FE-SEM and light microscopy This unique patterning of the bio-directed nanodeposition process can be also observed by imaging the deposited cellulose nanofibers using field emission-scanning electron microscopy (FE-SEM) correlated with the real time video analysis using light microscopy.

At first, light microscopic observations of the deposited fiber clarified that adherence to the molecular tracks occurred every 13.9 μm (SD = ±0.2 μm) as a mean distance along the orientation of the template as shown in the schematic figure of Fig. 2. Alternating with this parallel movement, the cell jumped off the tracks and detoured every 7.3 μm (SD = ±0.2 μm), until it became parallel to neighboring tracks, as also indicated in the schematic figure of Fig. 2. Once again soon jumping off, it repeated in the same manner until it stopped moving.

Fig. 3a shows a bacterium in contact with a nematic ordered chitin template that was moving in a waving fashion. During the moving pattern, it deposited a cellulose nanofiber that relatively flattened due to interaction with the nematic ordered chitin prior to the curving pattern in the movement. In the FE-SEM images of Figs. 3a and 3b, the dotted circle indicated the area where the interaction between the fiber and template occurred. Because of the contrast of the image, this was not clear compared with other areas of the fiber. Thus, such an interaction may be a trigger for a change in the running direction of the bacterial cell.

After the cell "jumped off" the tracks on the oriented chitin template, it still continued to secrete its cellulose ribbon, but now in

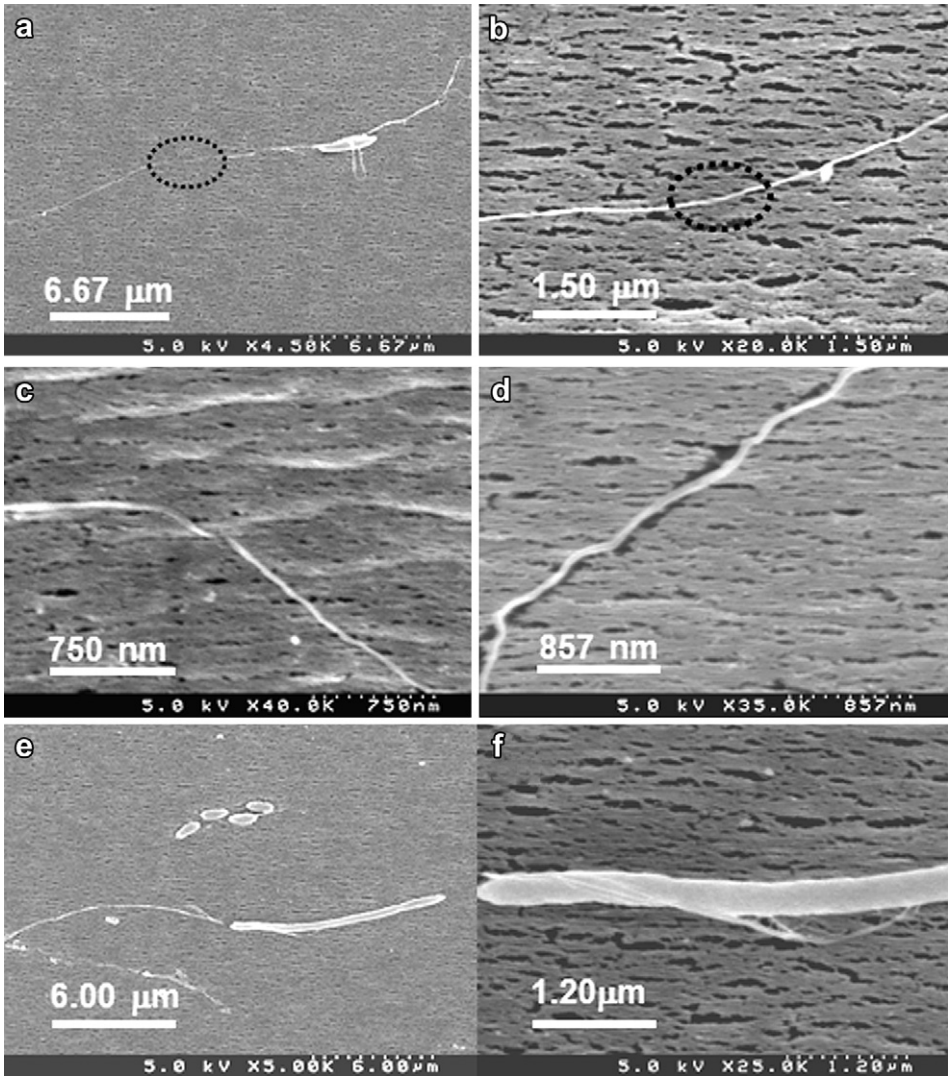

FIG. 3. FE-SEM images of the cellulose nanofiber deposition process. Examples of a–d on bacteria synthesizing cellulose nanofibers on the oriented molecular tracks of nematic ordered chitin template. Examples of e and f indicate self-rotation of a *Gluconacetobacter xylinus* cell.

the form of a twisted ribbon (Figs. 3c and 3d), which is the normal morphology when not in contact with an ordered substrate. This alternating pattern was observed to repeat as many as 20 times across the entire template.

G. xylinus usually rotates around the self-axis with secretion of a cellulose nanofiber, resulting in the twisted cellulose ribbon. In fact, Figs. 3c and 3d indicated this rotating movement that was an indication of interaction-free of the secreted fiber with the chitin template. Thus, Figs. 3e and 3f, which displayed winding fibers around the bacterium body, proves self-rotating of the bacterium cell during the detour following jumping off the tracks. Fig. 3f is the enlarged one of the cell in Fig. 3e. It is clear that the cell extruded the fiber with twisting, attributing to self-rotating of the cell. In this way, these results suggest that magnitude of interfacial interaction can regulate the waving pattern of bacterial movements and deposition of nanofibers, which leads to autonomous fabrication of 3-D structures with a unique pattern and a controlled growth direction of the product.

Effect of blending of cellulose with chitin as templates on patterning of fiber deposition and bacterial movements With the addition of cellulose as a component for nematic ordered chitin template, the molecular ordering was altered, as previously reported (6). In the previous report, we found that application of the preparative method for NOC to chitin and cellulose/chitin blends did not permit the formation of nematic ordered states like NOC on the molecular scale, but instead, induced a variety of hierarchical nematic ordered states on various scales. Details are given in Refs. (3,5,6). By the same preparation method for NOC, chitin molecules may be self-assembled to form a microfibril, and further the individual microfibrils tend to be parallel with the distance of 1.60 ± 0.21 nm, as shown in the TEM image of Fig. 1. The cellulose/chitin molecular aggregates in the stretched blend film are aligned similarly to nematic ordered chitin. Furthermore, it was expected to alter the magnitude of interfacial interactions that occurred with the microfibrils by addition of cellulose as a component.

To understand the present cases for chitin blends in comparison of the NOC, we employed WAXD measurements in order to determine the molecular ordering occurring with addition of cellulose. Fig. 4 shows WAXD intensity curves in both equatorial and meridional directions of the stretched chitin/cellulose blend films mixed at the desired ratio. There were two typical peaks that appeared at $2\theta = 9.3$ and 19.5 in the equatorial direction and three peaks at $2\theta = 16.5$, and 26.5 and 35.0° in the meridional direction, respectively for the chitin template. All the peaks appeared also for all the stretched chitin/cellulose blend films. This indicates that the formation of chitin microfibrils may be always induced by the stretching in the composite films. Though a peak at $2\theta = 9.3$ out of the two peaks at $2\theta = 9.3$ and 19.5 in the equatorial direction was apparently decreased by the addition of cellulose, the meridional reflections at $2\theta = 26.5$ did not exhibit a linear relation as with the above peak. However, the reflection peaks never shifted to be identical to NOC. Namely, the typical NOC structure is unique when prepared only using cellulose. These results indicate that the intermolecular interaction between cellulose and chitin may induce molecular aggregations leading to noncrystalline ordered domains, and they tend to be ordered parallel to the drawing axis. Then, it is assumed that a certain width of the ordered, but noncrystalline cellulose molecular aggregates may be located between the chitin microfibrils, depending on the composition of chitin/cellulose.

Fig. 5 shows the successive images showing the motion of a bacterium as it secreted a cellulose nanofiber using real time video analysis on the different amounts of cellulose as a component for nematic ordered chitin/cellulose blended templates of 50/50 and 25/75. In the two templates, the moving patterns were still waving. However, a remarkable difference appeared depending on the cellulose component ratio. The more cellulose was added, the less the amplitude became; namely getting close to a linear pattern. This is interpreted that more cellulose contained reduced the moving amplitudes into a straight manner. The moving rate for the individual blend ratios seemed to be within a non-significant range. The individual values are listed in Table 1.

Fig. 6 shows FE-SEM images of the cell and the deposited fibers depending on the cellulose ratios in the nematic ordered chitin/cellulose blend templates. Figs. 6a–c is for the template of 50/50 (chitin/cellulose), whereas Figs. 6d–g is for the template of 25/75 (chitin/cellulose). Both cases clearly show that the more cellulose added, the stronger interaction was engaged between the biosynthesized fibers and the template. On the chitin/cellulose (50/50) template, the deposited fiber was more fibrillated than that observed on the pure nematic ordered chitin template as shown in Figs. 3a–f. However, the cell itself still seemed to rotate judging from the twisted secreted fiber in the image of Fig. 6c. On the nematic ordered chitin/cellulose (25/75) containing more cellulose, there still was a waving pattern in the movement. However, the periodicity and the amplitude as listed in Table 1 was shorter. This shorter periodicity induces a more linear moving direction. Fig. 6f showing the deposited fiber on the chitin template reveals that the deposition manner indicated clearly a very strong interfacial interaction as

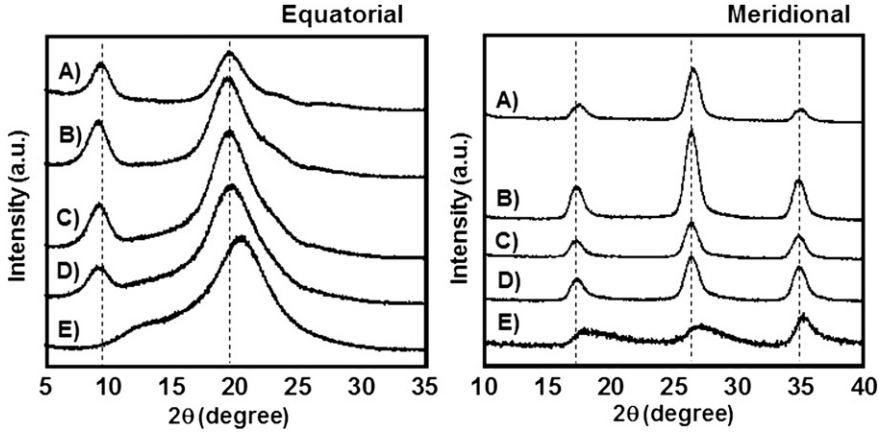

FIG. 4. Equatorial (left) and meridional (right) intensity curves of the WAXD for nematic ordered chitin and its blends with cellulose. "a.u." indicates arbitrary unit. Nematic ordered chitin/cellulose blends: (A) 100/0; (B) 67/33; (C) 50/50; (D) 33/77; (E) 0/100 (NOC).

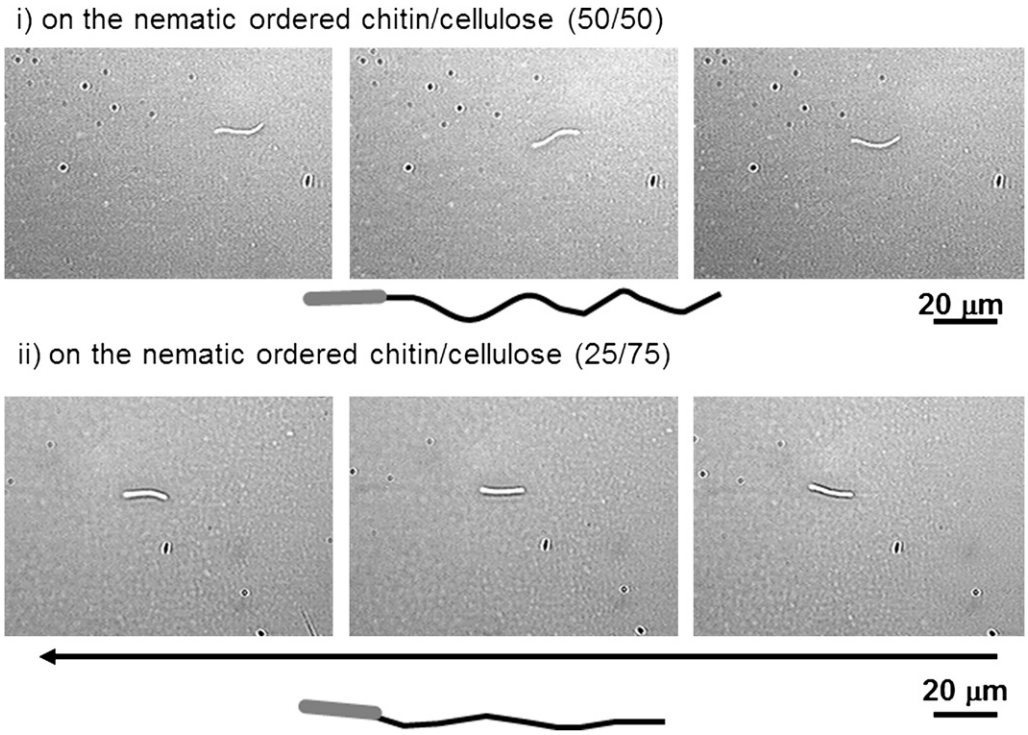

FIG. 5. Successive images by the normal bright field microscopic mode showing the motion of a bacterium using real time video analysis as it secretes a cellulose nanofiber on the nematic ordered chitin/cellulose blended templates (i) 50/50 and (ii) 25/75.

reported for that between NOC and the biosynthesized cellulose fiber (4). The flat fibrillated fiber was deposited on the template surface. *Gluconacetobacte*r secretes crystallized cellulose microfibrils directly into the culture medium from fixed enzyme complexes arranged in a row parallel to the long axis of the cell. The arrangement and position of the enzyme complexes determines the native hierarchical aggregation of the microfibrils including the polymer chains into the final crystalline nanofiber, an assembly of cellulose

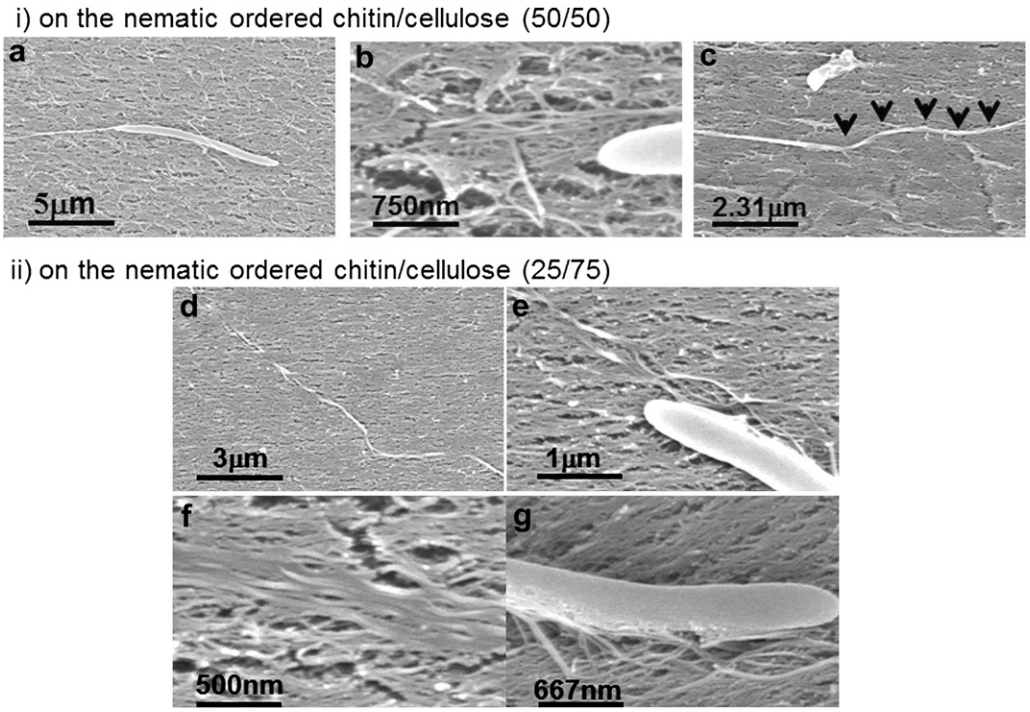

FIG. 6. FE-SEM images of the cellulose nanofiber deposition process. Panels a–c indicate bacteria synthesizing cellulose nanofibers on the oriented molecular tracks of nematic ordered chitin/cellulose blend (50/50) template. (i) Panels b and c indicate recently splayed cellulose nanofibers projecting from the cell and a deposited fiber, respectively. The rotation points of the cellulose fiber are indicated by the arrows in panel c. (ii) Images of d–g indicate bacteria synthesizing cellulose nanofibers on the oriented molecular tracks of nematic ordered chitin/cellulose blend (25/75) template. Images of f and g indicate the deposited fibers attached strongly with the template (f) and splayed cellulose nanofibers projecting from the cell (g), respectively.

sub-elementary fibrils. Figs. 6e and g indicated that the sub-elementary fibrils interacted with the surface as anchors to regulate the direction of the cell movement soon after the synthesis and prior to the self-assembly of them. These typical figures are compared with Figs. 3e and f of the cell and fiber deposited on the nematic ordered pure chitin template. Indeed, Figs. 6e–g of the images of a cell and the deposition of the fiber were very much like NOC cases as shown in Ref. 4. As described in the Introduction, the primary structure of chitin is different from that of cellulose only in the functional group of the C-2 position of the anhydroglucose unit. The acetamide group is replaced by the hydroxyl group, resulting in a large difference of favorability or magnitude in the induction of interaction engaged when the nematic ordered state is formed. In NOC, the C-2 positioned hydroxyl groups as well as C-6 positioned ones of the anhydroglucose unit in the cellulose molecules can create a unique characteristic of the molecular tracks. They are tightly adjacent to the surface and also aligned along the same axis like tracks, whereas the lateral order of the OH groups is not well coordinated. The OH groups as well as anhydroglucose units tend to be oriented as molecular tracks only in one direction across the entire NOC surface (3,5). Moreover, the patterned movements of the bacteria indicate a certain order on the template surfaces between chitin and cellulose. Considering the NOC surface structure (3,5), the ordered positional relationships of chitin and cellulose in the stretched composite templates is assumed to be a pair of the chitin microfibril and the neighboring cellulose molecular anhydroglucose ring plane that are facing alternately with each other. In addition, width of the parallel state for the paired aggregate may have a strong influence on the magnitude of the dynamic waving.

In summary, taking the difference in the substituent at the C-2 position of the anhydroglucose between cellulose and chitin into account, the OH groups at the C-2 position of anhydroglucose rings in primary structure of cellulose are the key to completely regulate the bacterial movements. The obtained results also suggest that the magnitude of the interfacial interaction between the template and the secreted nanofiber can regulate the pattern of bacterial movements and deposition of nanofibers, which leads to an autonomous fabrication of 3-D structures with a unique pattern and a controlled growth direction of the product.

ACKNOWLEDGMENTS

RMB received support from the Welch Foundation (F-1217) for part of this research. This study is partly supported by a Grant-in-Aid for Scientific Research (Nos. 22380099 and 23658146), Japan Society for the Promotion of Science.

References

1. **Drexler, K. E.:** Nanosystems: molecular machinery, manufacturing, and computation. Wiley Interscience, New York (1992).
2. **Taton, T. A.:** Bio-nanotechnology: two-way traffic, Nat. Mater., **2**, 73–74 (2002).
3. **Kondo, T., Togawa, E., and Brown, R. M., Jr.:** "Nematic ordered cellulose": a concept of glucan chain association, Biomacromolecules, **2**, 1324–1330 (2001).
4. **Kondo, T., Nojiri, M., Hishikawa, Y., Togawa, E., Romanovicz, D., and Brown, R. M., Jr.:** Biodirected epitaxial nanodeposition of polymers on oriented macromolecular templates, Proc. Natl. Acad. Sci. USA, **99**, 14008–14013 (2002).
5. **Kondo, T.:** Nematic ordered cellulose: its structure and properties, p. 285–306, in: Brown, R. M., Jr. and Saxena, I. M. (Eds.), Cellulose: molecular and structural biology. Springer, Dordrecht (2007).
6. **Kondo, T., Kasai, W., and Brown, R. M., Jr.:** Formation of nematic ordered cellulose and chitin, Cellulose, **11**, 463–474 (2004).
7. **Saito, Y., Okano, T., Chanzy, H., and Sugiyama, J.:** Structural study of α-chitin from the grasping spines of the arrow worm (*Sagitta* spp.), J. Struct. Biol., **114**, 218–228 (1995).
8. **Togawa, E. and Kondo, T.:** Change of morphological properties in drawing water-swollen cellulose films prepared from organic solutions: a view of molecular orientation in the drawing process, J. Polym. Sci. B: Polym. Phys., **37**, 451–459 (1999).
9. **Hestrin, S. and Schramm, M.:** Synthesis of cellulose by *Acetobacter xylinum*. 2. Preparation of freeze dried cells capable of polymerizing glucose to cellulose, Biochem. J., **58**, 345–352 (1954).
10. **Brown, R. M., Jr., Willison, J. H. M., and Richardson, C. L.:** Cellulose biosynthesis in *Acetobacter xylinum*: visualization of the site synthesis and direct measurement of the in vivo process, Proc. Natl. Acad. Sci. USA, **73**, 4565–4569 (1976).
11. **Tomita, Y. and Kondo, T.:** Influential factors to enhance the moving rate of *Gluconacetobacter xylinus* due to its nanofiber secretion on oriented templates, Carbohydr. Polym., **77**, 754–759 (2009).
12. **Minke, R. and Blackwell, J.:** The structure of α-chitin, J. Mol. Biol., **120**, 167–181 (1978).